ELSEVIER

Journal of Molecular Structure (Theochem) 630 (2003) 17–23

THEO CHEM

www.elsevier.com/locate/theochem

DFT and CASPT2 study of two thermal reactions of nitromethane: C–N bond cleavage and nitro-to-nitrite isomerization. An example of the inverse symmetry breaking deficiency in density functional calculations of an homolytic dissociation

J.F. Arenas, S.P. Centeno, I. López-Tocón, D. Peláez, J. Soto*

Department of Physical Chemistry, Faculty of Sciences, University of Málaga, E-29071-Málaga, Spain

Received 7 August 2002; accepted 15 November 2002

Abstract

The reaction paths of nitromethane leading to the dissociation products or isomerization to methyl nitrite have been computationally investigated at the CAS-SCF and DFT levels of theory. Additionally, the CAS-SCF wave functions were used as reference in a second-order perturbation treatment, CASPT2, in order to obtain a good estimate for the activation energy of each reaction path. Both methods predict the isomerization as a concerted reaction. However, the behavior of the two approximations with respect to dissociation is rather different; while CASPT2 predicts a barrier height of ($\approx$59 kcal/mol) in good accordance with the experimental activation energy (59.0 kcal/mol), B3-LYP/6-31G* calculations overestimate the barrier for more than 30 kcal/mol. The DFT prediction of the dissociation channel exhibits inverse symmetry breaking, dissociating to the unphysical absurd $CH_3^{\delta+}$ plus $NO_2^{\delta-}$.

Keywords: Nitromethane; Methyl nitrite; CAS-SCF; CASPT2; Density functional theory

1. Introduction

Thermal decomposition of nitro-compounds (R-NO_2), which occurs at rather low temperature, is of special relevance in the detonation of explosives [1]. Carbon–nitrogen bond breaking is the rate-limiting step in the thermolysis of such compounds [2,3]. The parent molecule of this family is nitromethane (CH_3NO_2), which has been extensively studied in the literature [4–10]. It was first predicted by theory [6], and then by experiments that unimolecular isomerization of nitromethane to methyl nitrite (CH_3ONO) competes with the thermal decomposition of nitromethane [4]. This same type of reaction has been found in other nitroderivatives as nitrobenzene [5].

Reaction mechanism of the thermolysis of nitromethane has been studied by other authors at different levels of theory [6–10]. These works have been mainly concerned with the relative height of barriers for the above mentioned reaction channels.

* Corresponding author. Tel.: +34-952-13-20-20; fax: +34-952-13-20-47.
E-mail address: soto@uma.es (J. Soto).

0166-1280/03/$ - see front matter © 2003 Elsevier Science B.V. All rights reserved.
doi:10.1016/S0166-1280(03)00165-9

Contention exists about the isomerization mechanism [8,9], that is, the nature of the transition state. If the C–N bond is completely broken before the C–O bond begins to form (loose transition state), the reaction can be described as the interaction of two radical fragments, $CH_3NO_2 \rightarrow CH_3 + NO_2 \rightarrow CH_3ONO$. In contrast, if the bond cleavage is not complete, a tighter transition state results and the reaction is described as $CH_3NO_2 \rightarrow CH_3ONO$. The aim of this work is to present a comparative study of the above mentioned reaction mechanisms by using two different levels of theory, CASPT2 and DFT, respectively.

2. Computational details

Geometries optimizations were carried out at the CAS-SCF level [11] with the MOLCAS 5.2 program [12] as well as using the density functional theory (DFT) with the B3-LYP [13,14] non-local exchange correlation functional as implemented in GAUSSIAN98 package of programs [15]. The 6-31G* basis sets of Pople et al. [16] and the atomic natural orbital basis sets (ANO-L) with the contraction scheme C,N,O (14s9p4d)/H(8s4p3d)//C,N,O [14s9p4d]/H[3s2p1d] have been used throughout this work. The minima and the transition states found in this work have been characterized by their analytic harmonic vibrational frequencies computed at the corresponding level of theory. Additionally, an IRC calculation [17] has been performed for the DFT transition state. Thus, the connection between the initial and final reaction products has been unambiguously established.

On the basis of the CAS-SCF optimized geometries, the energies of the critical points have been recomputed with the CASPT2 method [18]. Therefore, the CAS-SCF wavefunctions were used as reference in the second-order perturbation treatment, keeping frozen the 1s electrons of the carbon and nitrogen atoms, respectively, as determined in the CAS-SCF calculations.

The active space comprises 14 electrons distributed in 11 orbitals. These orbitals (Fig. 1) were visualized with the program MacMolPlt [19]. They include all the valence electrons excepting those corresponding to the C–H bonds.

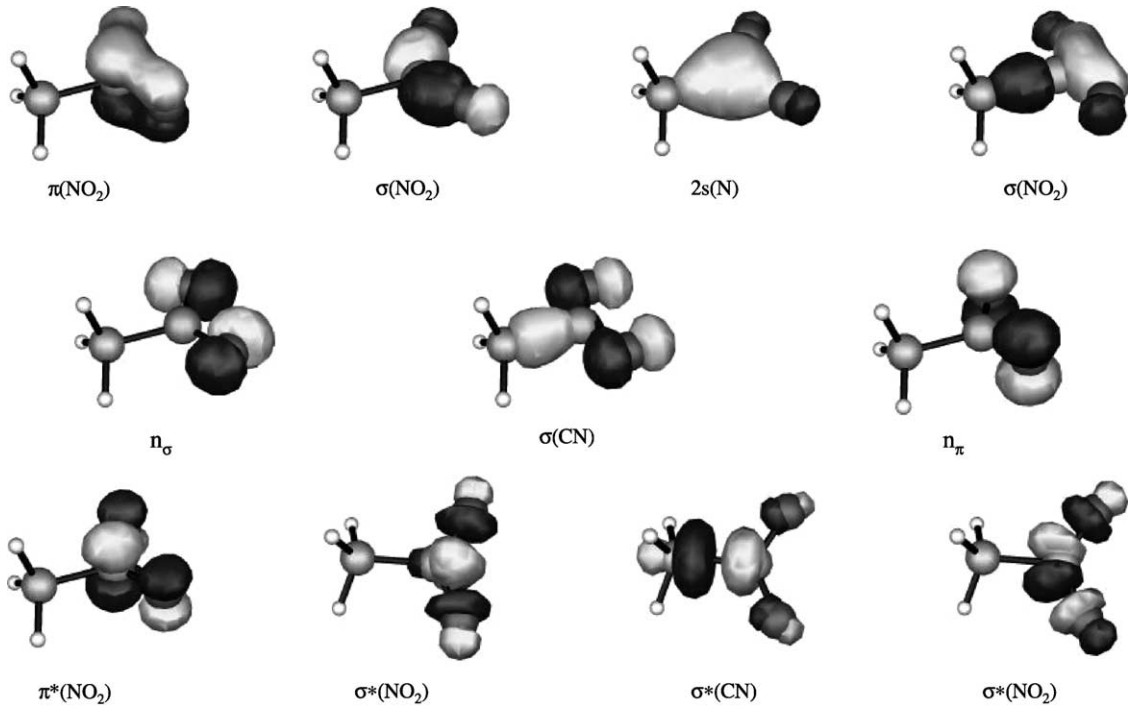

Fig. 1. CAS-SCF/6-31G* molecular orbitals of nitromethane.

The choice of the active space deserves some comments. This selection is straightforward if we want to study the dissociation channel leading to nitrogen dioxide (NO_2) formation. For this triatomic molecule, it has been demonstrated by Blahous III et al. [20] that the minimal active space, which ensures a free symmetry breaking wavefunction, must comprise 13 electrons in 10 orbitals. Therefore, the active space of nitromethane will include 14 electrons distributed in 11 orbitals; the additional orbital with respect to NO_2 comes from the σCN bond. Nevertheless, in order to accelerate the calculation, we have tried to use a smaller active space by excluding the σNO and σ^*NO molecular orbitals, which gives an active space of 10 electrons in 7 orbitals. Unfortunately, the wavefunction did not converge free of symmetry breaking with this smaller active space.

3. Results and discussion

The C_s geometries of nitromethane (NM) and *trans*-methyl nitrite (MN) are shown in Fig. 2, which includes also the C_1 transition state (TS1) connecting them. The imaginary frequencies of the transition mode at three different levels of theory are 846*i* (B3-LYP/6-31G*), 1063*i* (CAS-SCF/6-31G*), and 1063*i* (CAS-SCF/ANO-L), respectively. The structural parameters are collected in Table 1, and their energies in Table 2. The DFT geometrical parameters of the stable isomers are closer to the experimental values [21,22]. The IRC calculation (Fig. 3) clearly shows that this reaction path leads to the *trans*-isomer. Both methods predict quite similar barrier heights (70 kcal/mol, 6-31G* basis sets) for isomerization, which differ significantly from the value of 55.5 kcal/mol deduced from IRMPD experiments [4]. However, it is pointed out in Ref. [8] that this experimental value may be too low due to an underestimation of the *A* factor for the nitro-to-nitrite rearrangement. In fact, our best estimation (CASPT2/ANO-L) of the isomerization barrier gives 62.4 kcal/mol. Equally, both levels of theory (DFT and CASPT2) agree with the tight character of the transition state. Therefore, a single step reaction with a partial charge on each moiety (B3-LYP/6-31G*, $NO_2^{-0.37}$; CASPT2/6-31G*, $NO_2^{-0.39}$; CASPT2/ANO-L, $NO_2^{-0.45}$) is predicted for the isomerization channel.

The energy profiles of the interpolation lines (DFT and CASPT2) leading asymptotically to the dissociation products are plotted in Fig. 4. There is no stationary structure which could be assigned to the transition state for the dissociation path. These curves start at the optimized geometries of nitromethane and finish at the optimized structures of the isolated fragments ($CH_3 + NO_2$) when the C–N distance is 4.0 Å. The CASPT2 asymptotic limit (≈59.0 kcal/mol) agrees nicely with the experimental activation energy (59.0 kcal/mol [23]). On the other hand, the energy of the isolated fragments at the B3-LYP/

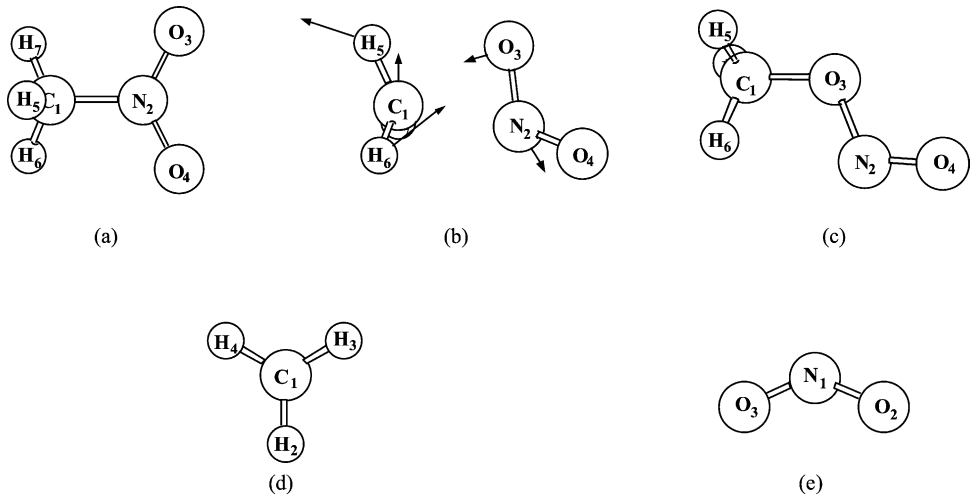

Fig. 2. Optimized geometries of the critical points on the potential energy surfaces for dissociation and isomerization.

Table 1
Structural parameters of nitromethane (NM), transition state (TS1) and *trans*-methyl nitrite (MN)

	NM			TS1		MN		
	CAS	DFT	Exp [a]	CAS	DFT	CAS	DFT	Exp [b]
dC1N2	1.520 (1.524)	1.499	*1.489*	1.944 (1.948)	1.943	2.364	2.345	
dC1O3	2.349 (2.349)	2.329		2.031 (2.032)	2.002	1.455	1.431	*1.435*
dN2O3	1.230 (1.224)	1.227	*1.224*	1.329 (1.326)	1.299	1.447	1.427	*1.451*
dN2O4	1.230 (1.224)	1.227	*1.224*	1.211 (1.203)	1.204	1.184	1.180	*1.170*
dC1H5	1.080 (1.079)	1.092	*1.088*	1.071 (1.069)	1.085	1.080	1.094	*1.099*
dC1H6	1.077 (1.075)	1.088	*1.088*	1.073 (1.069)	1.086	1.080	1.094	*1.099*
dC1H7	1.077 (1.075)	1.088	*1.088*	1.070 (1.071)	1.082	1.080	1.094	*1.099*
aO3N2C1	117.0 (117.0)	117.0	*117.4*	74.0 (74.0)	73.3	35.6	34.9	
aC1O3N2	35.2 (35.3)	35.0		67.0 (67.2)	68.3	109.1	110.3	
aO4N2C1	117.0 (117.0)	117.0	*117.4*	152.6 (151.1)	155.4	146.2	145.7	
aH5C1N2	106.9 (106.2)	106.8	*107.2*	118.9 (98.5)	120.4	122.0	122.4	
aH6C1N2	107.7 (107.7)	108.0	*107.2*	91.9 (118.2)	92.0	74.7	75.0	
aH7C1N2	107.7 (107.7)	108.0	*107.2*	98.7 (91.1)	96.6	121.9	122.4	
DhO4N2C1O3	−178.3 (180.0)	−178.1		−122.3 (−121.5)	−123.5	0.0	0.0	
DhH5C1N2O3	89.2 (−90.0)	89.1		32.3 (−93.0)	25.1	75.1	75.6	
DhH6C1N2H5	119.2 (119.0)	118.8		119.0 (125.4)	119.6	104.8	104.4	
DhH7C1N2H5	−119.2 (−119.0)	−118.8		−125.5 (−115.7)	−125.1	−150.4	−151.3	

Calculated parameters with the 6-31G* basis set; between parenthesis ANO-L values.
[a] Ref. [21].
[b] Ref. [22].

6-31G* level amounts to 62 kcal/mol. However, the DFT interpolation overestimates the exit channel for more than 30 kcal/mol. Additionally, the charges of the fragments along the interpolation lines, obtained from the Mulliken population analysis, are given in the same figure as an inset. We obtain two uncharged radicals (homolytic dissociation) at the CASPT2 level, as it is observed experimentally. In contrast, at

Table 2
Energetic of the critical points on the potential energy surface of nitromethane (NM) and methyl nitrite (MN)

Geometry	CAS-SCF	CASPT2	DFT	ΔE [a]
NM	−243.84394	−244.31623	−245.00933	0.0; 0.0 [b]
	(−243.94920) [c]	(−244.54510)		(0.0) [d]
TS1	−243.73139	−244.20389	−244.89918	70.5; 69.1
	(−243.83838)	(−244.44559)		(62.4)
MN	−243.84623	−244.31106	−245.00543	3.2; 2.4
NO_2 [e]	−204.20749	−204.55006	−205.07221	–
	(−204.29200)	(−204.58000)		
CH_3 [f]	−39.55449	−39.67043	−39.83829	–
	(−39.57496)	(−39.73281)		
($CH_3 + NO_2$) [g]	−243.76202	−244.22138	−244.85456	59.5; 97.1
	(−243.86733)	(−244.45121)		(58.9)

6-31G* basis sets.
[a] Relative energy (kcal/mol) with respect to the minimum of nitromethane.
[b] In Italic DFT energy.
[c] In parenthesis, ANO-L values.
[d] In parenthesis ANO-L energy.
[e] CAS(13e,10o).
[f] CAS(1e,1o).
[g] Asymptotic limit (4 Å).

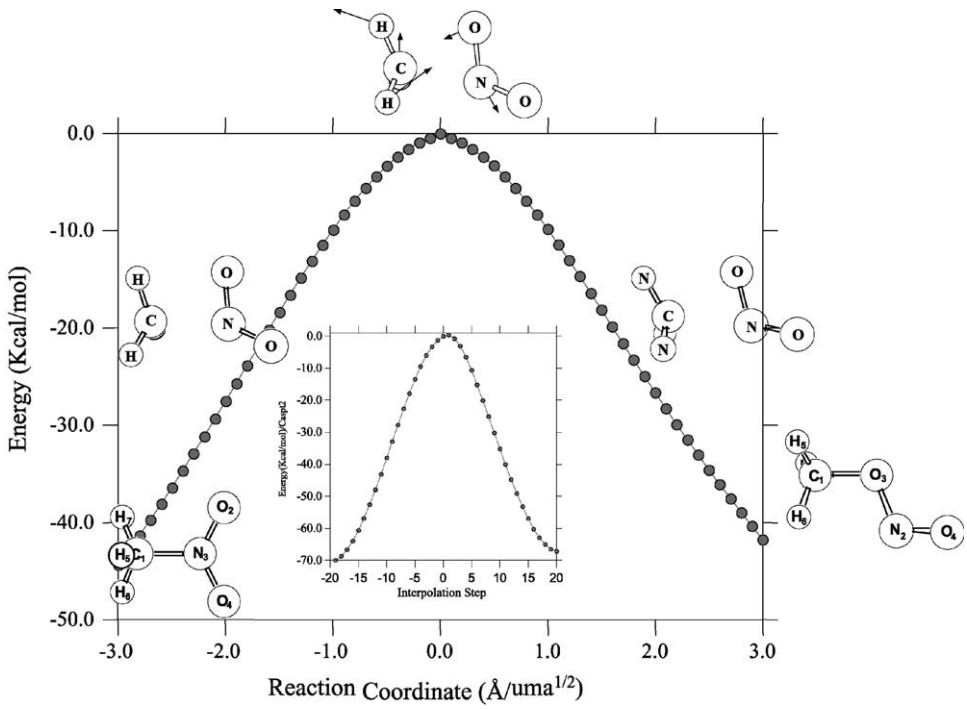

Fig. 3. B3-LYP/6-31G* IRC for $CH_3NO_2 \rightarrow CH_3ONO$ isomerization. The inset corresponds to the CAS-SCF interpolation going from nitromethane to methyl nitrite.

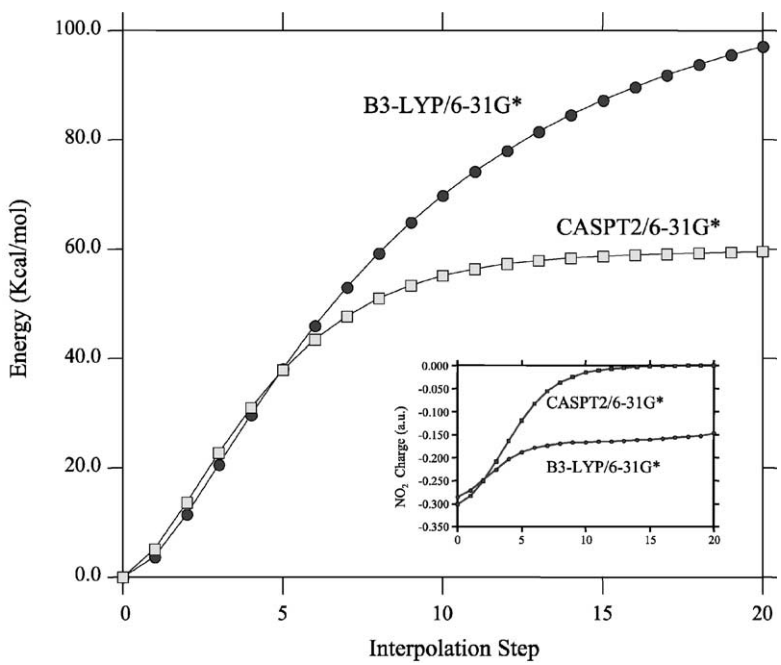

Fig. 4. Interpolation lines (B3-LYP and CASPT2) for the dissociation reaction. The inset corresponds to the charge of the NO_2 fragment along the interpolation line.

the B3-LYP/6-31G* level, each fragment gain a spurious fractional charge, even at rather long distances between them. Bally and Sastry first described this abnormal dissociation behavior of the density functional methods in 1997 [24], and it was named 'inverse symmetry breaking'. Inverse symmetry breaking has been reported as a common phenomenon for the DFT results for radical ions with two equivalent fragments (see for example Refs.[24,25]). As pointed out by Xie et al. [25], inverse symmetry breaking may be an inherent character of the non-HF DFT exchange functionals, yielding a physically incorrect picture of the potential energy surfaces. The name of this artifact comes from the fact that the charge localization of the density functional approximation contrasts with that obtained from some SCF methods when symmetry breaking is present. While the symmetry breaking deficiency of the SCF methods localizes the charge in one of the dissociating fragments, inverse symmetry breaking favors an incorrect delocalized electron density distribution.

4. Conclusions

In summary, the thermal dissociation of nitromethane and its nitro-to-nitrite rearrangement have been studied at the DFT and CASPT2 levels of theory. Whereas both methods agree in their predictions for the isomerization channel, [one step reaction (CH_3-$NO_2 \rightarrow CH_3ONO$)], their behaviors in the dissociation path are rather different; the DFT results are affected by the inverse symmetry breaking deficiency. The calculations show that, independently of the level of theory applied, the dissociation path is preferred over the isomerization channel. With respect to the nature of the transition state for the rearrangement path, our results are closer to the tight transition state computed at the HF/6-31G* level which was reported by Mckee in 1986 [7]. The previously published [8,9] loose transition states seem to be artifacts; the latter due to the very small active space used, and the former because of the symmetry breaking effect which is present in that calculation. To finish, it is worthy to note that the minimal active space, which describes in a balanced way both the dissociation and isomerization reactions of nitromethane, must comprise 14 electrons distributed in 11 orbitals. However, it was not possible to move on the potential energy surface from TS1 to MN by using the larger ANO-L basis sets in conjunction with such an active space.

Acknowledgements

This research has been supported by the Ministerio de Ciencia y Tecnología of Spain under the project BQU2000-1353. The authors thank D.R. Larrosa for the technical support in running the calculations and SCAI (University of Málaga) for using an Origin 2000 SGI computer.

References

[1] A. Gindulyte, L. Massa, L. Huang, J. Karle, J. Phys. Chem. A 103 (1999) 11040.
[2] R. Guirgis, D. Hsu, D. Boga, E. Oran, Combust. Flame 61 (1985) 51.
[3] J.F. Arenas, J.I. Marcos, J.C. Otero, A. Sánchez-Gálvez, J. Soto, J. Chem. Soc. Faraday Trans. 92 (1996) 363.
[4] (a) A.M. Wodtke, E.J. Hintsa, Y.T. Lee, J. Phys. Chem. 90 (1986) 3549. (b) A.M. Wodtke, E.J. Hintsa, Y.T. Lee, J. Chem. Phys. 82 (1986) 1044.
[5] A.C. González, C.W. Larson, D.F. McMillen, D.M. Golden, J. Phys. Chem. 89 (1986) 4809.
[6] M.J.S. Dewar, J.P. Ritchie, J. Alster, J. Org. Chem. 50 (1985) 1031.
[7] M.L. Mckee, J. Am. Chem. Soc. 108 (1986) 5784.
[8] M.L. Mckee, J. Phys. Chem. 93 (1989) 7365.
[9] R.P. Saxon, M. Yoshimine, Can. J. Chem. 70 (1992) 572.
[10] M.R. Manaa, L.E. Fried, J. Phys. Chem. A 102 (1998) 9884.
[11] (a) B.O. Roos, in: K.P. Lawley (Ed.), Advances in Chemical Physics; Ab Initio Methods in Quantum Chemistry—II, Wiley, Chichester, England, 1987, pp. 399, Chap. 69. (b) J. Hinze, J. Chem. Phys., 59, 1973, pp. 6424.
[12] K. Andersson, M. Barysz, A. Bernhardsson, M.R.A. Blomberg, Y. Carissan, D.L. Cooper, M. Cossi, T. Fleig, M.P. Fülscher, L. Gagliardi, C. de Graaf, B.A. Hess, G. Karlström, R. Lindh, P.-Å. Malmqvist, P. Neogrády, J. Olsen, B.O. Roos, B. Schimmelpfennig, M. Schütz, L. Seijo, L. Serrano-Andrés, P.E.M. Siegbahn, J. Stålring, T. Thorsteinsson, V. Veryazov, M. Wierzbowska, P.-O. Widmark, MOLCAS Version 5.2, Lund University, Sweden, 2001.
[13] A.D. Becke, J. Chem. Phys. 98 (1993) 5648.
[14] C. Lee, W. Yang, R.G. Parr, Phys. Rev. B 37 (1988) 785.
[15] M.J. Frisch, G.W. Trucks, H.B. Schlegel, G.E. Scuseria, M.A. Robb, J.R. Cheeseman, V.G. Zakrzewski, J.A. Montgomery,

Jr., R.E. Stratmann, J.C. Burant, S. Dapprich, J.M. Millam, A.D. Daniels, K.N. Kudin, M.C. Strain, O. Farkas, J. Tomasi, V. Barone, M. Cossi, R. Cammi, B. Mennucci, C. Pomelli, C. Adamo, S. Clifford, J. Ochterski, G.A. Petersson, P.Y. Ayala, Q. Cui, K. Morokuma, D.K. Malick, A.D. Rabuck, K. Raghavachari, J.B. Foresman, J. Cioslowski, J.V. Ortiz, A.G. Baboul, B.B. Stefanov, G. Liu, A. Liashenko, P. Piskorz, I. Komaromi, R. Gomperts, R.L. Martin, D.J. Fox, T. Keith, M.A. Al-Laham, C.Y. Peng, A. Nanayakkara, C. Gonzalez, M. Challacombe, P.M.W. Gill, B. Johnson, W. Chen, M.W. Wong, J.L. Andres, C. Gonzalez, M. Head-Gordon, E.S. Replogle, J.A. Pople, Gaussian 98, Revision A.7, Gaussian, Inc., Pittsburgh, PA, 1998.

[16] (a) R. Ditchfield, W.J. Hehre, J.A. Pople, J. Chem. Phys. 54 (1971) 724. (b) W.J. Hehre, R. Ditchfield, J.A. Pople, J. Chem. Phys. 56 (1972) 2257. (c) P.C. Hariharan, J.A. Pople, Theor. Chim. Acta 28 (1973) 213.

[17] (a) C. Gonzalez, H.B. Schlegel, J. Chem. Phys. 90 (1989) 2154. (b) C. Gonzalez, H.B. Schlegel, J. Phys. Chem. 94 (1990) 5523.

[18] (a) K. Andersson, P.-Å. Malmqvist, B.O. Roos, A.J. Sadlej, K. Wolinski, J. Phys. Chem. 94 (1990) 5483. (b) K. Andersson, P.-Å. Malmqvist, B.O. Roos, J. Chem. Phys. 96 (1992) 1218. (c) K. Andersson, B.O. Roos, D.R. Yarkony,Advances Series in Physical Chemistry; Modern Electron Structure Theory vol. 2World ScientificSingapore (1995) 55 part I.

[19] B.M. Bode, M.S. Gordon, J. Mol. Graphics and Modeling 16 (1999) 133.

[20] C.P. Blahous III, B.F. Yates, Y. Xie, H.F. Schaefer III, J. Chem. Phys. 93 (1990) 8105.

[21] A.P. Cox, S. Waring, J. Chem. Soc. Faraday Trans. 2 (1972) 1060.

[22] B.J. van der Veken, R. Maas, G.A. Guirgis, H.D. Stidham, T.G. Sheehan, J.R. Durig, J. Phys. Chem. 94 (1990) 4029.

[23] H.E. O'Neal, S.W. Benson, Kinetic Data on Gas Phase Unimolecular Reactions, 1970, NSRDS-NB521, Washington, DC.

[24] T. Bally, G.N. Sastry, J. Phys. Chem. A 101 (1997) 7923.

[25] Y. Xie, H.F. Schaefer III, X.-Y. Fu, R.-Z. Liu, J. Chem. Phys. 111 (1999) 2532.